DRAFT VERSION FEBRUARY 5, 2008
Preprint typeset using LaTeX style emulateapj v. 12/14/05

TROJAN PAIRS IN THE HD 128311 AND HD 82943 PLANETARY SYSTEMS?

KRZYSZTOF GOŹDZIEWSKI[1]
Toruń Centre for Astronomy, N. Copernicus University, Gagarina 11, 87-100 Toruń, Poland

MACIEJ KONACKI[2]
Nicolaus Copernicus Astronomical Center, Polish Academy of Sciences, Rabiańska 8, 87-100 Toruń, Poland
Department of Geological and Planetary Sciences, California Institute of Technology, MS 150-21, Pasadena, CA 91125, USA
Draft version February 5, 2008

ABSTRACT

Two nearby stars, HD 128311 and HD 82943, are believed to host pairs of Jupiter-like planets involved in a strong first order 2:1 mean motion resonance (MMR). In this work we reanalyze available radial velocity (RV) measurements and demonstrate that it is also possible to explain the observed RV variations of the parents stars as being induced by a pair of Trojan planets (i.e., in a 1:1 MMR). We show that these Trojan configurations reside in extended zones of stability in which such systems may easily survive in spite of large masses of the planets, large eccentricities and nonzero mutual inclinations of their orbits. We also show that HD 82943 could harbor a previously unknown third planet of $\sim$0.5 Jupiter masses in $\sim$ 2 AU orbit.

Subject headings: celestial mechanics, stellar dynamics—methods: numerical, N-body simulations—planetary systems—stars: individual (HD 82943, HD 128311)

1. INTRODUCTION

Follow-up radial velocity (RV) observations of Sun-like stars with planets have revealed a number of extrasolar multi-planet systems. Many of them are involved in low-order mean motion resonances (MMRs). In particular, at least four extrasolar systems are involved in a strong first order 2:1 MMR: Gliese 876 (Marcy et al. 2001), HD 82943 (Mayor et al. 2004), HD 128311 (Vogt et al. 2005), and HD 73526 (Tinney et al. 2006). A considerable effort has been devoted to study the origin (Kley 2003; Kley et al. 2004) and dynamical stability of these intriguing systems (e.g., Goździewski & Maciejewski 2001; Lee & Peale 2002; Ji et al. 2003; Beaugé & Michtchenko 2003; Lee 2004; Psychoyos & Hadjidemetriou 2005; Ferraz-Mello et al. 2005; Lee et al. 2006). Yet dynamical studies of the resonant configurations often rely on the 2-Keplerian coplanar fits by the discovery teams. It has been demonstrated that the 2-Keplerian models can be of a very limited use for systems involved in strong mutual interactions (e.g., Laughlin & Chambers 2001; Rivera & Lissauer 2001; Goździewski et al. 2005). Even if a model incorporates mutual interactions, due to typically short time-span and a limited number of the observations, the orbital inclinations are barely constrained and usually only coplanar, edge-on configurations are considered. However, the recent results of Thommes & Lissauer (2003) and Adams & Laughlin (2003) suggest that a significant fraction of planetary systems involving giant planets may be substantially non-coplanar. Dynamical mechanisms which lead to fast amplification of the relative inclination are especially effective in the first order resonance configurations (Thommes & Lissauer 2003). Also dynamical relaxation and collisional scattering of the protoplanets may favor large relative inclinations in such systems, even if they initially emerge in a flat protoplanetary disk.

The interpretation of the RV data for multi-planet system may be difficult. The determination of the number of planets and their orbital periods can be problematic for some systems. In particular, for those involved in a 1:1 MMR. A periodogram of the RV signal for such a system (Laughlin & Chambers 2002) is basically indistinguishable from that of a single planet in an eccentric orbit or, as we show in this paper, from a periodogram of a 2:1 MMR orbital configuration. Laughlin & Chambers (2002) and Nauenberg (2002) have demonstrated that a coplanar 1:1 MMR of Jovian planets may be stable in a wide range of their orbital parameters. The results of hydrodynamic simulations by Laughlin & Chambers (2002) indicate that Trojan planets in tadpole or horseshoe orbits might readily form and migrate within a proto-planetary disk. Presumably, a 1:1 configuration may also emerge as a result of dynamical relaxation or migration frequently used to explain 2:1 MMR configurations. In the Solar System there exist a number of moons involved in this type of resonance — famous Janus-Epimetheus system (co-orbital moons of Saturn, exchanging orbits), Helene-Polydeuces (Trojans of Dione, a moon of Saturn), Telesto–Calypso (Trojan moons of Tethys, yet another moon of Saturn). Dynamically, these configurations mimic planetary systems in the 1:1 MMR.

In this paper, we perform an independent analysis of the RV data for HD 128311 and HD 82943 to verify if the observed RV variations can be explained not only by a configuration in a 2:1 MMR but also 1:1 MMR. The inevitable problem with modeling such systems is that due to a limited number of data and relatively large measurement errors, the best-fit orbital elements often and easily lead to catastrophically unstable configurations. In order to solve this problem one needs a method of fitting which incorporates a stability criterion. Without such a constraint, one can find a stable best-fit orbits basically by chance. When we deal with a 1:1 MMR configuration, an appropriate stability control is essential as the planets share the same (or a very similar) orbit and a multi-parameter dynamical model is highly nonlinear. In this paper we use the term "Trojan planets" not only for tadpole, close to coplanar and circular configurations but for all configurations characterized by a 1:1 MMR so having not only similar semi-major axes but also (possibly) large relative inclinations

[1] e-mail: k.gozdziewski@astri.uni.torun.pl
[2] e-mail: maciej@ncac.torun.pl

and variable eccentricities.

2. NUMERICAL APPROACH

Due to strong mutual interactions, the planetary systems with giant planets have to avoid the unstable zones of the MMRs, a proximity of the collision zone and the zone of global instability where the overlapping of MMRs occurs. Otherwise, the chaotic diffusion quickly leads the planets to collisions between each other or with the parent star. The overall picture of the phase space of a planetary system is predicted by the fundamental Kolmogorov-Arnold-Moser theorem (Arnold 1978): the phase space is not continuous with respect to the stability criterion. Hence, commonly used (in particular, gradient-like) algorithms of exploring the phase space are poorly designed for this task because they are "blind" to a sophisticated fractal-like structure of the phase space.

The KAM stability is described in terms of stable (regular, quasi-periodic) and unstable (chaotic) motions. At first, the use of such a formal criterion in the fitting process may be problematic. Almost any planetary system, including our own, can be very close to a chaotic state. Nevertheless, we expect that even if chaos appears, it should not impair the astronomical stability (Lissauer 1999) meaning that a system is bounded over a very long time and any collisions or ejections of planets do not occur. However, for configurations involving Jupiter-like companions in close orbits with large eccentricities, the formal stability seems to be well related to the astronomical stability of the system, i.e., chaotic motions mean a fast destabilization of a planetary configuration over short-time scale related to the most significant, low-order MMRs. It has been already demonstrated by dynamical analysis of systems residing in the regions of the phase space where the low-order MMRs are possible (e.g. Goździewski & Maciejewski 2001; Goździewski et al. 2005, 2006). We should note that there is not known any general relation between the Lyapunov time (a characteristic time-scale of the formal instability) and the event time (the time after which a physical change of a planetary system happens; see, e.g. Lecar et al. 2001; Michtchenko & Ferraz-Mello 2001). To put these ideas into action and to search for stable best-fit solutions in a self-consistent and optimal fashion, we treat the dynamical behavior (in terms of chaotic and regular or mildly-chaotic states) as an additional observable at the same level of importance as the RV measurements. This powerful approach has been already described in detail and successfully applied in Goździewski et al. (2003, 2005, 2006).

The kernel of our approach is the the genetic algorithm scheme (GA) implemented by Charbonneau (1995) in his publicly available[3] code PIKAIA. The GAs are ideal for our purpose because of their global non-gradient nature and their proven ability to efficiently explore a multidimensional noncontinuous parameter space. The RV data are modeled by a synthetic signal of the full N-body dynamics (Laughlin & Chambers 2001). The $(\chi^2_\nu)^{1/2}$ function is modified by a stability penalty term employing an efficient fast indicator MEGNO (Goździewski et al. 2003). The GA fits are finally refined by yet another very accurate non-gradient minimization scheme by Nelder and Mead (Press et al. 1992) widely known as the simplex method. This greatly reduces the CPU usage. We give the algorithm an acronym GAMP (Genetic Algorithm with MEGNO Penalty).

The simplex method finds local minima of $(\chi^2_\nu)^{1/2}$. The code may be also trapped in resonance islands surrounded by strongly chaotic motions even if $(\chi^2_\nu)^{1/2}$ inside such islands is larger than in the neighboring (but unstable) areas. By collecting solutions to which the GAMP converged in many independent runs, we gather an ensemble of the local best-fit solutions. It helps us to illustrate the multidimensional properties of $(\chi^2_\nu)^{1/2}$ and to obtain realistic estimates of the parameter's errors by choosing the solutions within prescribed limits of the overall best-fit $(\chi^2_\nu)^{1/2}$ found in the entire search. At the end, some of the selected best fits can be refined with longer integration times and much lower simplex tolerance than is used during the search phase.

Finally, the stability of the best-fit solutions is examined in planes of selected orbital osculating elements using the Spectral Number method (*SN*) by Michtchenko & Ferraz-Mello (2001). It is an efficient fast indicator completely independent on MEGNO. This enables us to verify and illustrate the best-fit solutions in a robust way and to examine dynamical properties of such configurations in wide ranges of neighboring initial conditions. Note that the *SN* is related here to the short-term dynamics. Thus the spectral signal analyzed is a time series $\{f(t) = a(t)\exp[\mathrm{i}\lambda(t)]\}$ where $a(t)$ and $\lambda(t)$ are respectively an osculating *canonical* semi-major axis and longitude of a planet. Such an analysis makes it possible to resolve the proper mean motion n as one of the fundamental frequencies of the system. Note also that a stability criterion in the GAMP code may be basically arbitrary. We use the formal KAM criterion as the most general and well defined one.

3. HD 128311

The HD 128311 is an active K0 star (Vogt et al. 2005). In the discovery paper, Butler et al. (2003) found an indication of a Jovian planet and a linear trend in the RV data. They concluded that due to photospheric activity ($\log R'_{\rm HK} \simeq -4.4$) the stellar jitter is large ~ 20 m/s and the signal variability may be explained exclusively by the jitter. Using an updated set of 76 RV measurements, Vogt et al. (2005) found that the observations can be modeled by a system of two Jupiter-like planets involved in a 2:1 MMR. The current estimate of the stellar jitter by these authors is ~ 9 m/s but still uncertain with a 50% error. We rescale the measurement errors by adding this estimate in quadrature to the formal RV errors.

The discovery team reports that the best-fit 2-Keplerian model yielding $(\chi^2_\nu)^{1/2} = 1.86$ and an rms ~ 18 m/s is catastrophically unstable. Using our hybrid GA/simplex code (Goździewski & Migaszewski 2006) driven by the Keplerian model of the RV, we found a different, apparently better 2-planet solution which has $(\chi^2_\nu)^{1/2} = 1.717$ and an rms $=$ 15.16 m/s. The model parameters $(K, P, e, \omega, T_{\rm p} - T_0)$, i.e., the semi-amplitude, orbital period, eccentricity, the argument of periastron and the time of periastron passage, for this fit are as follows: (51.948 m/s, 459.870 d, 0.362, 59.401°, 2474.867 d) and (77.214 m/s, 917.371 d, 0.248, 5.541°, 2310.806 d) for the inner and outer planet, respectively; $T_0 =$ JD 2,450,000 and the velocity offset $V_0 = 1.011$ m/s. It is argued that the fit parameters of a multi-planet system should be interpreted in terms of osculating Keplerian elements and minimal masses related to the Jacobi coordinates (Lee & Peale 2003). Adopting the date of the first observation as the osculating epoch, we recalculated the inferred *astrocentric* osculating elements $(m_p \sin i, a, e, \omega, M)$ as follows (1.639 m_J, 1.101 AU, 0.362, 59.37°, 272.79°) and (3.194 m_J, 1.746 AU, 0.249, 5.39°, 199.62°) for the inner and outer planet, respectively. Still,

[3] http://www.hao.ucar.edu/Public/models/pikaia/pikaia.html

the derived configuration is also unstable and disrupts during about 200,000 yr. Nevertheless, we found that its MEGNO signature is characteristic for a system residing on the border of a stable region rather than a collisional configuration. Thus one may suspect that in its proximity, a rigorously stable solutions can be easily found.

In order to deal with the problem of an unstable 2-Kepler fit, Vogt et al. (2005) applied a method of fitting which incorporates the mutual interaction between planets (Laughlin & Chambers 2001) and, additionally, explicitly involves stability criterion. As such the authors use the maximal eccentricity attained by the companions during an integration time. They report many stable solutions corresponding to the 2:1 MMR. According to the authors, their best fit yields an rms ~ 14.7 m/s and $(\chi^2_\nu)^{1/2} \sim 1$. We could not reproduce that value of $(\chi^2_\nu)^{1/2}$. The quoted $(\chi^2_\nu)^{1/2}$ could be misprinted or a jitter estimate larger than ~ 9 m/s was used in the calculations.

For a comparison with that result and as a background for a further analysis, we performed the GAMP search for the best-fit solution to the RV data from Vogt et al. (2005) assuming that a 2:1 resonance is indeed present in the coplanar and edge-on system. We also explored a more general model in which the orbits are mutually inclined but we did not find substantially better fits.

In Fig. 1, the elements of the best-fit solutions from the GAMP runs are shown in a few representative planes of the osculating elements at the date of the first observation, JD, 2,450,983.827. In the GAMP code, the MEGNO was evaluated over $1000 - 5000$ orbital periods of the outer planet that is both efficient enough and makes it possible to withdraw strongly chaotic, unstable solutions. The best-fit initial conditions are marked with symbols of different sizes — larger circles indicate a smaller $(\chi^2_\nu)^{1/2}$ (a better fit). Only *stable* solutions within the 3σ confidence interval of the best-fit solution (given in Table 1) are shown. In overall, the statistics of initial conditions shown in Fig. 1 is in accord with the results of Vogt et al. (2005), see their Fig. 12. The permitted *initial* eccentricities of the fits span skewed and narrow valley in the (e_b, e_c)-plane. Let us note that we represent the N-body initial conditions in terms of astrocentric, osculating Kepler elements at the epoch of the first observation.

The orbital elements for the outer planet have larger errors than for the inner one. Both semimajor-axes and phases are already very well determined. The parameters of the stable best-fit solution are given in Table 1 (Fit I). Note that this strictly regular solution has $(\chi^2_\nu)^{1/2} \simeq 1.731$ and rms $\simeq 15.28$ m/s. A very similar value of $(\chi^2_\nu)^{1/2}$ in the N-body and Keplerian fits means that the mutual interactions between planetary companions are not evident in the Doppler signal spanning 10 yr. Nevertheless, we stress that the stability constraints are essential for obtaining stable configuration of the N-body model.

In Figure 2, we show the stability analysis the best fit solution corresponding to a 2:1 MMR (Fit I given in Table 1). The Spectral Number, $\log SN$, as well as $\max e_{b,c}$, the maximal eccentricities of both planets, and $\max\theta$, the maximal $\theta = \varpi_b - \varpi_c$ (where $\varpi_{b,c}$ are the longitudes of pericenters), attained during the integration over $\sim 7 \cdot 10^4$ orbital periods of the outer body are shown in Figure 2. It turns out that the best-fit solution lies on the border of an island related to the corotation of apsides (θ as well as the critical arguments of the 2:1 MMR are librating about 0° with a large amplitude). The border of the stable resonance zone which is present in the SN-map can be also seen in all other maps, in particular in the $\max e$-maps. This is a strong argument that the formal stability criterion is in the one-to-one relationship with the behavior of the system. Clearly, the search zone for the best-fit solution should be limited to the resonance island which constantly changes its shape when we change the orbital parameters. Thanks to the instability penalty in our approach, we have confidence that the obtained solution is indeed optimal (i.e., it minimizes $(\chi^2_\nu)^{1/2}$ and is dynamically stable).

In our next test, we carried out a search for a stable Trojan configuration. Our model was extended to 14 osculating orbital elements including the inclinations and one nodal longitude as free parameters. Note that due to very similar orbital semi-major axes, the planets are numbered by giving the symbol "b" to that planet which has a smaller initial eccentricity. As one can see in Fig. 3, a well defined minimum of $(\chi^2_\nu)^{1/2}$ is present in the (a_b, a_c) and (e_b, e_c) planes. The best-fit inclinations are not very well constrained nevertheless their concentration is quite evident, in spite of a moderate time span of the observations.

The osculating elements of the best-fit solution are given in Table 1 (Fit II). Its $(\chi^2_\nu)^{1/2} \simeq 1.797$ and rms $\simeq 15.48$ m/s are very close to those of the 2:1 MMR configuration. The synthetic RV signals of both solutions are shown in Fig. 4. They can be barely distinguished one from another. We also computed the Lomb-Scargle periodograms of both synthetic signals and we plotted them together with the periodogram of the data set in Fig. 5. It shows that periodograms of the 2:1 and 1:1 configurations almost perfectly match each other. It would be very difficult to distinguish between the configurations by looking only at the periodograms.

The best-fit Trojan configuration resides in a wide stable zone in the plane of the eccentricities which extends up to 1 for both of these elements (see Fig. 6). The resonance area in the (a_c, e_c)-plane covers about 0.2 AU. This width is even larger than for the 2:1 MMR configuration (see Fig. 2). Obviously, the stable 1:1 MMR is possible due to the corotation of the apsides seen in the $\max\theta$-maps (θ librates about 180^0).

Our choice of the stability criterion enables us to obtain very sharp borders of the resonance area. If this criterion was violated, the system would quickly disrupt (because both e go to 1). In Fig. 7 we show the stability maps for a solution which has an rms of about 15.7 m/s (slightly more than the best one) and corresponds to much smaller masses (both initial inclinations are about 45^o). Essentially, all the dynamical features of the system do not change but the width of the resonance zone shrinks substantially. This is also an argument that an appropriate stability criterion has to be an integral part of the fitting tool. Due to an extremely nonlinear nature of the system, even a small change of its initial elements may lead to a significant change in the shape of the resonance zone. Simultaneously, $\max e$ becomes very "flat" in the regions of large e — so $\max e$ would not be a convenient stability indicator in a GAMP-like code. Another argument is that the variable rate of the chaotic diffusion which leads to the changes of the eccentricity can be sometimes to small to detect a collision or a qualitative change of the configuration over relatively short integrations which, for efficiency reasons, have to be limited to the time-scale of the MMRs. One might think that (again, mainly for efficiency reasons) $\max\theta$ would be a better choice than both $\max e$ and MEGNO as a stability criterion. However, that test may also fail as in the resonance zone the critical angle θ may librate about different centers (usually, about

of 0° or 180°) but it can circulate in some marginally unstable regions as well (see Appendix for details).

4. HD 82943

The HD 82943 planetary system (Mayor et al. 2004) has drawn attention of many researchers (e.g., Goździewski & Maciejewski 2001; Ji et al. 2003; Ferraz-Mello et al. 2005; Lee et al. 2006). The 2-Keplerian solutions produced by the discovery team correspond to catastrophically unstable configurations (Goździewski & Maciejewski 2001; Ferraz-Mello et al. 2005; Lee et al. 2006). The discovery team did not publish the observations of HD 82943 in source form. The method of dealing with the problem of unavailable RV data relies on digitizing the published figures depicting the measurements. This somewhat unusual approach has already become an accepted procedure (e.g., Goździewski & Maciejewski 2001; Goździewski & Konacki 2004; Ferraz-Mello et al. 2005; Lee et al. 2006).

First, we digitized 142 data points from the figures of Mayor et al. (2004). They slightly differ from the real observations. In particular, it is difficult to recover the exact moments of the observations (Ferraz-Mello et al. 2005) but such digitized measurements still properly describe the overall shape of the observed RV curve and its characteristic features. We also graphically derived the measurement errors and rescaled them by adding in quadrature the stellar jitter which we estimated as ~ 5 m/s on the basis of (Wright 2005).

Having such "measurements", we recovered the best-fit 2-Kepler solutions published by the discovery team (Mayor et al. 2004). The only problem seems to be a little larger value of the rms of $\simeq 7.1$ m/s (compared to 6.8 m/s quoted in the original work). Using the digitized RV measurements, Ferraz-Mello et al. (2005) showed that stable 2:1 MMR configurations are possible. Their orbital parameters of coplanar, edge-on systems are similar to those we found with GAMP (Fit III in Table 1). We note that these authors looked for the best-fit solutions by minimizing the rms rather than $(\chi^2_{\rm v})^{1/2}$, and they did not increased the internal errors by jitter. Also the discovery team did not account for the jitter in their solutions.

We extended the search for the best-fit solution assuming that a 1:1 MMR can be present in the HD 82943 system. As in the previous case, we did not find any stable and strictly coplanar, edge-on configuration of this type. However, using the generalized model in which masses, inclinations and one nodal longitude are free parameters, we found many stable solutions. Their quality is not as good as for the 2:1 MMR — the best 1:1 MMR fit has $(\chi^2_{\rm v})^{1/2} \simeq 1.2$ and the rms is $\simeq 8.1$ m/s which is about of 1 m/s worse than for our best 2:1 MMR solution. Still, the 1:1 MMR solution may be plausible (note that we use digitized "observations"). Also, since the mass of the parent star cannot be determined precisely (Ferraz-Mello et al. 2005), and when new measurements are available, the best-fit parameters and their $(\chi^2_{\rm v})^{1/2}$ may change. We demonstrate it in the next section.

The best-fit 1:1 MMR configuration (Fit IV in Table 1) is characterized by initially large mutual orbital inclination because, although the inclinations for both planets are almost the same, the nodal longitude is about 180° (and the apsidal lines are anti-aligned). The orbital evolution leads to quite large variations of the orbital inclinations (a few tens of degrees). The stability maps shown in Figure 8 reveal that, apparently, such a system would be locked in an extremely large zone of stable motions which extends up to $e_{\rm b,c} \sim 1$. This means that the eccentricities could reach extremely large values but the system would be still stable. The width of the resonance with respect to $a_{\rm c}$ is also relatively large, about 0.2 AU. A zone of strictly periodic motions can be seen in the map for $\max\theta$, close to its diagonal.

4.1. *Fits for HD 82943 revisited*

We extended the analysis of HD 82943 after gaining access to the same data set used by Lee et al. (2006) (and also Lee 2005, private communication). These authors also used the "digitized" measurements from Mayor et al. (2004) but added new observations obtained with the Keck/HIRES. These new very accurate data fill in some gaps in the CORALIE measurements as well as significantly increase the time span of the observations. For consistency with Lee et al. (2006) we adopted the jitter estimate of 4.2 m/s.

The results of fitting 2-planet Keplerian models and the analysis of their stability by Lee et al. (2006) strongly confirm the possibility of a stable 2:1 MMR in the HD 82943 system. Still, new questions may be asked. The best fit of the 2:1 MMR configuration yields an rms ~ 8 m/s which is unexpectedly larger by 1 m/s from that quoted for the CORALIE data by the discovery team Mayor et al. (2004) as well as by Ferraz-Mello et al. (2005), and in this work.

For the updated data set, we recovered all the best fit Keplerian solutions quoted by Lee et al. (2006) using our GA/simplex code. Some of them appear to be formally chaotic or strongly unstable. Thus we searched for a stable N-body solution using GAMP assuming that the velocity offsets for the CORALIE and Keck/HIRES data are independent. The found best-fit, *rigorously stable* solution corresponding to the 2:1 resonance of an edge-on system is given in Table 2 (Fit V). Its quality is not very different from the best solutions found by Lee et al. (2006) but the initial eccentricities are significantly different. Our Fit V is most similar to the 2-planet Kepler Fit II of Lee et al. (2006). We also found other solutions which are similar to their Fit III and IV with respect to small initial $e_{\rm c}$.

According to the results of Ferraz-Mello et al. (2005) and Lee et al. (2006), $e_{\rm c}$ and $\omega_{\rm c}$ are the less constrained parameters of the Kepler fits to the RV data of HD 82943. Thus we computed dynamical maps for the relevant solutions (see Fig. 9 and its caption) as well as for Fit II of Lee et al. (2006). These maps reveal two narrow zones of stability in which the best-fit solutions reside. All acceptable (stable) 2:1 MMR fits likely belong to these two distinct islands. We label them with A and B in Fig. 9. Note that the positions and shape of the resonance areas are significantly altered when the fit parameters are adjusted. Inside the resonance zone A, the amplitudes of the critical angles may vary in wide ranges. Lee et al. (2006) found that their Fit II has very small amplitudes of the critical angles of the 2:1 MMR, $\sim 10^\circ$. Our best N-body fit V yields much larger amplitudes, $\sim 40^\circ$. The large amplitudes of the critical angles are also reported by Ferraz-Mello et al. (2005). The resonance island A is characterized by the corotation of apsidal lines. We found that in this zone $\max\theta$ may be very close to the libration center 0°. For instance, for the dynamical map of Fit V, at $(e_{\rm c} \sim 0.116, \omega_{\rm c} \sim 127.7^\circ)$ the variations of $\max\theta < 2^\circ$, indicating a strictly periodic solution. In the second island labeled by B in Fig. 9, $\max\theta$ also librates about 0° but with large amplitudes.

We may speak about dynamical similarity of the best-fit solutions found so far, having in mind their position in the two

resonance zones. The results of the dynamical analysis done by Lee et al. (2006) and in this paper favor the 2:1 MMR fits located in the island A (about $\omega_c \sim 120^\circ$). This zone is extended with respect to the not well constrained e_c and very small amplitudes of the 2:1 MMR critical angles are possible.

We also found many stable mutually inclined configurations using the orbital inclinations and one nodal argument as free parameters. Still, all these fits have the rms ~ 8 m/s. By releasing the stability requirements in the GAMP code, one finds the best 2-planet fit yielding the rms ~ 7.5 m/s (Fit VII in Table 2). However, this configuration disrupts in a few hundred years. Curiously, such a solution involves a brown dwarf and a Jovian planet on inclined orbits (mutual inclination of $\sim 80^\circ$).

In fact, our main goal was to perform a possibly extensive search for 1:1 configurations. The statistics of stable solutions gathered in this search is illustrated in Fig. 10, in a similar manner as for HD 128311 system. Qualitatively, the solutions do not differ from the ones we found using the CORALIE data only. The semi-major axes and the eccentricities are very well constrained. Also the initial inclinations and masses are bounded to two well determined local minima of $(\chi^2_v)^{1/2}$. The best fit solution is given in Table 2 (Fit VI). Its rms ~ 8.4 m/s is even closer to that of the 2:1 MMR best fit than in the case of the CORALIE data alone. Its MEGNO signature which indicates perfectly stable, quasi-periodic configuration, and the evolution of orbital elements during 3 Myr are shown in Fig. 11. The relevant dynamical maps of the best fit in the (e_b, e_c)- and (a_c, e_c)-plane are shown in Fig. 12. We also compared periodograms (Fig. 13) of the synthetic curves for the 2:1 MMR, 1:1 MMR and the measurements (shown in Fig. 14). Also in this case the periodograms for the 2:1 and 1:1 MMR perfectly match each other.

4.2. *The third planet in HD 82943?*

The solutions described so far do not explain the curious rms excess that is present in the extended data set. It seems unlikely the problem is caused by some inconsistency of the measurements from the two spectrographs. Another possible explanation is that there is a new, unknown object in the system. That possibility is suggested by Lee et al. (2006). Looking at their Fig. 4 which shows the residual signal to the 2-planet solutions, we can see a quasi-sinusoidal modulation with the period about of 1000 d. Yet the jitter estimates of HD 82943 are uncertain by 50% (Lee et al. 2006). Thus by adopting values as high as 6–7 m/s, one would obtain $(\chi^2_v)^{1/2} \sim 1$ and the larger rms would be not necessarily unreasonable. Still, the hypothesis about the third planet is a very attractive explanation of the rms excess. Below we try to find out whether such a configuration would be consistent with a stable dynamics.

First, we searched for 3-planet solutions using the hybrid Kepler code and "blindly" assuming the same bounds of the orbital periods of [10,1200] d and eccentricities of [0,0.8] for every planet. The use of multi-planet Keplerian model enables us to quickly localize regions of orbital parameters in which potentially stable, N-body fits can be found. The code was restarted thousands of times. In this search the algorithm converged to a few distinct local minima yielding similar rms and $(\chi^2_v)^{1/2}$.

Remarkably, two of the Keplerian best fits, yielding $(\chi^2_v)^{1/2} \sim 1.2$ and an rms ~ 7 m/s correspond to *coplanar* configurations involving two (of three) Jovian planets in 1:1 MMR. The primary parameters (K, e, P, ω, T_0) of these fits are given in Table 3 (Fit X and Fit XI, respectively). Their planets c and d would have similar periods but the eccentricities of the two outer planets in 1:1 MMR are significantly different. Unfortunately, these fits are highly unstable. We did not succeed in "stabilizing" them by GAMP; nevertheless, the search was not very extensive and we suspect that stable solutions involving mutually inclined orbits may exist.

The Fit IX (the mathematically best fit found in this paper) yields $(\chi^2_v)^{1/2} = 1.08$ and an rms ~ 6.38 m/s that indicates a almost "perfect" solution. It could be interpreted as a configuration of the outermost planet accompanying the confirmed giants involved in the 2:1 MMR. Unfortunately, this solution is very unstable due to a large eccentricity of the outermost planet. We tried to refine it with GAMP. In the relevant range of semi-major axes we found stable solutions, and the one we selected is given as Fit VIII in Table 2. Let us note that the stability criterion forces e_d of this solution to a small value ~ 0.02 which also increases the rms to about 7.35 m/s. The dynamical maps shown in Fig. 15 reveal narrow islands of stability in which the solution is found. The MEGNO signature (the left-upper panel of Fig. 16) uncovers a weakly chaotic nature of this solution. Nevertheless, there is no sign of a physical instability over at least 250 Myr (Fig.16 is for the initial 5 Myr integration period). A peculiarity of this fit is that e_d remains small in spite of a close proximity to the two larger companions in eccentric orbits. For a comparison with the previously found 1:1 MMR and 2:1 MMR solutions, the synthetic curve of Fit VIII is shown in the bottom panel of Fig. 14.

The described results might indicate that our knowledge of HD 82943 system is still limited in spite of much effort devoted to study the RV data of the parent star. The currently available measurements permit many qualitatively different orbital solutions well fitting the measurements. Still, the use of stability criterion in the fit process seems to be essential to resolve the degeneracy between very good but strongly unstable Keplerian and Newtonian fits which, as we have shown above, can easily appear.

5. CONCLUSIONS

We have demonstrated the RV measurements for HD 128311 and HD 82943 harboring 2-planet systems may be successfully modeled with two qualitatively different orbital configuration. One is already recognized configuration corresponding to a 2:1 MMR. We show that these observations are equally well modeled with Trojan pairs of planets (a 1:1 MMR). Both these types of orbital configurations produce very similar periodograms of the RV signal. A common feature of the Trojan solutions for both systems is the possibility for large eccentricities of the orbits, reaching ~ 0.8. Still, the best-fit Trojan configurations reside in extended zones of rigorously stable quasi-periodic motions. The ease of maintaining stability and the large zones of regular motions may strengthen the hypothesis about the 1:1 MMR configurations.

It is difficult to explain finding two systems in a 1:1 MMR in the sample of only ~ 20 multi-planet systems. A most promising mechanism that might produce such a configuration is the dynamical relaxation and planetary scattering (Adams & Laughlin 2003). In particular, an argument supporting such a hypothesis for the HD 82943 system is the evidence of a planet engulfment by the parent star (Israelian et al. 2001). That event indicates planetary scaterring in the past.

However, its effect on the currently observed configuration of the system would be hard to predict. To the best of our knowledge there are no works that could explicitly explain an inclined 1:1 MMR configuration as a result of a migration. On the other hand, the origin of the 2:1 MMR is a well recognized problem as we know of at least four systems presumably involved in such a resonance. Our work demonstrates that the 1:1 MMR configurations can be used to describe the observations of HD 128311 and HD 82943 . This hopefully will encourage others to study the origin of such systems.

The best-fit Trojan configurations were found using of our approach of modeling the RV data which incorporates a stability indicator. For this purpose we use a formal KAM criterion which is closely related to a physical behavior of a planetary system. This criterion generalizes the $\max e$ and $\max\theta$ maps. Still, these maps help us to determine the character of motions — e.g. a type of the corotation of the apsides. Obviously, all the three indicators are strictly related. Presumably, the stability maps would change if the model of motion included the relativistic and tidal interactions with the star. Although these factors are orders of magnitude smaller than the leading gravitational interactions, their influence might change the overall stability picture of the systems. Our work on this subject is ongoing.

6. ACKNOWLEDGMENTS

We appreciate discussions with Prof. Sylvio Ferraz-Mello and his help with obtaining the RV data of the HD 82943 system. We thank Dr. Man Hoi Lee for a detailed review, critical remarks that improved the manuscript and for providing the full set of RV measurements of HD 82943. This work is supported by the Polish Ministry of Education and Science, Grant No. 1P03D 021 29. M.K. is also supported by NASA through grant NNG04GM62G.

APPENDIX

Here we discuss the problem of a proper choice of the stability indicator in a GAMP-like fitting code. We analyze two 1:1 initial conditions for the HD 82943 system which are marked in the stability maps (Fig. 8, the upper row; one is our best-fit 1:1 MMR configuration). Let us recall that the calculations of *SN* were conducted over $3\cdot10^4$ orbital periods of the planets (about of $6\cdot10^4$ yr). Apparently, both initial conditions are localized in an extended resonance zone. Figure 17 (upper row) illustrates the temporal MEGNO, $Y(t)$, as a function of time but computed over a much longer time-span, $2.5\cdot10^5$ orbital periods. For the best-fit solution, the behavior of $Y(t)$ (oscillations about 2) corresponds to a strictly quasi-periodic system while a slow divergence of this indicator can be observed for the modified initial condition (marked with a diamond in the *SN* map, Fig. 8). It indicates that in this case the system is in fact weakly chaotic (the Lyapunov exponent is relatively small, $\sim 10^{-5}$ yr^{-1}). An inspection of the $\max\theta$-map for this initial condition reveals that θ in this case circulates (Fig. 8 and Fig. 17, right column) but on the average the apsides are anti-aligned and this helps to maintain the stability. It means that $\max\theta$ would not be a good choice as a stability indicator. Nevertheless, it is a valuable tool for resolving the complex structure of the resonance.

REFERENCES

Adams, F. C. & Laughlin, G. 2003, Icarus, 163, 290
Arnold, V. I. 1978, Mathematical methods of classical mechanics (Graduate texts in mathematics, New York: Springer, 1978)
Beaugé, C. & Michtchenko, T. A. 2003, MNRAS, 341, 760
Butler, R. P., Marcy, G. W., Vogt, S. S., Fischer, D. A., Henry, G. W., Laughlin, G., & Wright, J. T. 2003, ApJ, 582, 455
Charbonneau, P. 1995, ApJS, 101, 309
Ferraz-Mello, S., Michtchenko, T. A., & Beaugé, C. 2005, ApJ, 621, 473
Goździewski, K., Konacki, M., & Maciejewski, A. J. 2006, ApJ, (in press, arXiv:astro-ph/0511463)
Goździewski, K. & Konacki, M. 2004, ApJ, 610, 1093
Goździewski, K., Konacki, M., & Maciejewski, A. J. 2003, ApJ, 594
—. 2005, ApJ, 622, 1136
Goździewski, K. & Maciejewski, A. 2001, ApJ, 563, L81
Goździewski, K. & Migaszewski, C. 2006, A&A, 449, 1219
Israelian, G., Santos, N. C., Mayor, M., & Rebolo, R. 2001, Nature, 411, 163
Ji, J., Kinoshita, H., Liou, L., Nakai, H., & Li, G. 2003, ApJ, 591, L57
Ji, J., Liu, L., Kinoshita, H., Zhou, J., Nakai, H., & Li, G. 2003, Celestial Mechanics and Dynamical Astronomy, 87, 113
Kley, W. 2003, Celestial Mechanics and Dynamical Astronomy, 87, 85
Kley, W., Peitz, J., & Bryden, G. 2004, A&A, 414, 735
Laughlin, G. & Chambers, J. E. 2001, ApJ, 551, L109
—. 2002, AJ, 124, 592
Lecar, M., Franklin, F. A., Holman, M. J., & Murray, N. J. 2001, ARA&A, 39, 581
Lee, M. H., 2004, ApJ, 611, 517
Lee, M. H., Butler, R. P., Fischer, D. A., Marcy, G. W., & Vogt, S. S. 2005, ApJ, apJ preprint doi:10.1086/500566
Lee, M. H. & Peale, S. J. 2002, ApJ, 567, 596
—. 2003, ApJ, 592, 1201
Lissauer, J. J. 1999, Rev. Mod. Phys., 71, 835
Marcy, G., Butler, R., Fischer, D., Vogt, S., Lissauer, J., & Rivera, E. 2001, ApJ, 556, 296
Mayor, M., Udry, S., Naef, D., Pepe, F., Queloz, D., Santos, N. C., & Burnet, M. 2004, A&A, 415, 391
Michtchenko, T. & Ferraz-Mello, S. 2001, ApJ, 122, 474
Nauenberg, M. 2002, AJ, 124, 2332
Press, W. H., Teukolsky, S. A., Vetterling, W. T., & Flannery, B. P. 1992, Numerical Recipes in C. The Art of Scientific Computing (Cambridge Univ. Press)
Psychoyos, D. & Hadjidemetriou, J. D. 2005, Celestial Mechanics and Dynamical Astronomy, 92, 135
Tinney *et al.* 2006, arXiv:astro-ph/0602557
Thommes, E. W. & Lissauer, J. J. 2003, ApJ, 597, 566
Rivera, E. W. & Lissauer, J. J. 2001, ApJ, 402, 558
Vogt, S. S., Butler, R. P., Marcy, G. W., Fischer, D. A., Henry, G. W., Laughlin, G., Wright, J. T., & Johnson, J. A. 2005, ApJ, 632, 638
Wright, J. T. 2005, PASP, 117, 657

TABLE 1
The best-fit 2-planet initial conditions for the HD 128311 (Vogt et al. 2005) and HD 82943 Mayor et al. (2004) planetary systems found with GAMP (MEGNO was calculated over $\simeq$ 1000–5000 periods of the more distant companion). Jitter estimates are 9 m/s for HD 128311 and 5 m/s for HD 82943 . Astrocentric osculating elements are given for the date of the first observation from Vogt et al. (2005) and Mayor et al. (2004), respectively. The masses of the parent stars are of 0.84$M_\odot$ for HD 128311 and of 1.15 $M_\odot$ for HD 82943 .

	Fit I		Fit II		Fit III		Fit IV	
	HD 128311 (2:1 MMR)		HD 128311 (1:1 MMR)		HD 82943 (2:1 MMR)		HD 82943 (1:1 MMR)	
Orbital parameter	**b**	**c**	**b**	**c**	**b**	**c**	**b**	**c**
$m_2 \sin i$ [M_J]	1.606	3.178	7.174	6.954	1.810	1.812	9.888	4.182
a [AU]	1.112	1.732	1.737	1.796	0.744	1.192	1.187	1.201
e	0.359	0.214	0.311	0.599	0.395	0.128	0.504	0.658
i [deg]	90.00	90.00	44.22	16.96	90.00	90.00	19.23	19.57
ω [deg].....	71.58	12.71	84.14	112.53	121.25	222.94	123.74	126.33
Ω [deg]	0.0	0.0	209.79	0.0	0.0	0.0	178.52	0.0
$M(t_0)$ [deg]	271.72	190.23	125.24	311.56	355.99	258.96	356.02	170.30
V_0 [m/s]	0.970		0.655		-0.761		-2.877	
$(\chi^2_\nu)^{1/2}$	1.731		1.797		1.047		1.221	
rms [m/s]	15.28		15.49		7.12		8.13	

TABLE 2
The best-fit 2-planet initial conditions for the HD 82943 planetary system, on the basis of data set used by Lee et al. (2006). The stable fits are found with GAMP (MEGNO was calculated over $\simeq$ 1000–5000 periods of the more distant companion). Jitter estimate is 4.2 m/s. Astrocentric osculating elements are given for the date of the first observation from Mayor et al. (2004). The mass of the parent star is 1.15 $M_\odot$. CORALIE RV data are shifted by 8128.598 m/s.

	Fit V (stable)		Fit VI (stable)		Fit VII (unstable)		Fit VIII (stable)		
	HD 82943 (2:1 MMR)		HD 82943 (1:1 MMR)		HD 82943 (2:1 MMR)		HD 82943 (3-planet)		
Orbital parameter	**b**	**c**	**b**	**c**	**b**	**c**	**b**	**c**	**d**
$m_2 \sin i$ [M_J]	1.461	1.728	2.043	3.932	17.16	1.761	1.679	1.867	0.487
a [AU]	0.748	1.186	1.208	1.180	0.751	1.240	0.751	1.197	2.125
e	0.448	0.268	0.640	0.500	0.380	0.001	0.386	0.110	0.018
i [deg]	90.00	90.00	49.35	56.56	6.260	87.85	90.0	90.0	90.0
ω [deg].....	126.82	138.35	133.92	127.88	119.84	187.81	118.08	144.47	114.61
Ω [deg]	0.0	0.0	145.71	0.0	346.23	0.0	0.0	0.0	0.0
$M(t_0)$ [deg]	359.23	336.85	186.39	353.84	0.00	286.03	2.65	345.24	79.76
V_0 [m/s]	13.66		12.41		15.42		14.60		
V_1 [m/s]	-7.72		-6.86		-4.96		-0.73		
$(\chi^2_\nu)^{1/2}$	1.39		1.45		1.32		1.27		
rms [m/s]	7.98		8.40		7.58		7.36		

TABLE 3
Primary best-fit parameters of the 3-planet Kepler models found in this paper on the basis of RV measurements of HD 82943 used by Lee et al. (2006). The epoch T_0 is JD 2,450,000. The adopted jitter estimate is 4.2 m/s. CORALIE RV measurements are shifted by 8128.598 m/s. All fits are dynamically unstable.

	Fit IX			Fit X			Fit XI		
	HD 82943 (3-planet)			HD 82943 (3-planet)			HD 82943 (3-planet)		
Parameter	**b**	**c**	**d**	**b**	**c**	**d**	**b**	**c**	**d**
K [m/s]	59.735	41.838	10.493	55.926	16.997	36.487	51.173	19.853	36.059
P [d]	219.423	442.893	937.663	219.766	417.579	445.914	219.536	418.197	449.093
e	0.398	0.141	0.580	0.403	0.712	0.061	0.437	0.683	0.210
ω [deg]	107.386	86.565	215.039	120.701	240.476	100.133	119.385	236.421	97.881
T_p [JD-T_0] .	1842.338	232.810	384.940	2505.152	2141.264	3819.642	3163.810	1722.905	1585.272
$(\chi^2_\nu)^{1/2}$	1.079			1.183			1.180		
rms [m/s] ..	6.37			6.97			7.01		
V_0 [m/s] ...	-3.80			-8.90			-8.65		
V_1 [m/s] ...	17.06			16.99			16.77		

FIG. 1.— The best fits obtained by the GAMP algorithm for the RV data published in Vogt et al. (2005) for HD 128311. In the model, the coplanar system and 2:1 MMR is assumed. Parameters of the fit are projected onto the planes of osculating orbital elements. The smallest filled circles are for the solutions with $(\chi^2_{\rm v})^{1/2}$ within the formal 3σ confidence interval of the best-fit solution, with $(\chi^2_{\rm v})^{1/2} < 1.79$. Bigger open circles are for $(\chi^2_{\rm v})^{1/2} < 1.761$ and $(\chi^2_{\rm v})^{1/2} < 1.741$ (2σ and 1σ confidence intervals of the best-fit solution, respectively). The largest circles are for the solutions with $(\chi^2_{\rm v})^{1/2} < 1.732$ marginally larger than $(\chi^2_{\rm v})^{1/2} = 1.731$ of the best-fit initial condition (Fit I, Table 1). A curve in the $(a_{\rm c}, e_{\rm c})$-plane denotes the planetary collision line which is determined from the relation $a_{\rm b}(1+e_{\rm b}) = a_{\rm c}(1-e_{\rm c})$ with $a_{\rm b}, e_{\rm b}$ fixed at their best-fit values. The nominal position of the 2:1 MMR inferred from the Kepler law is also marked.

FIG. 2.— The stability maps in the $(a_{\rm c}, e_{\rm c})$-plane in terms of the Spectral Number, $\log SN$, $\max e$ and $\max\theta$, for the best-fit solution corresponding to the putative 2:1 MMR for the coplanar HD 128311 system (see Table 1, Fit I). Colors used in the $\log SN$ map classify the orbits — black indicates quasi-periodic, regular configurations while yellow strongly chaotic systems. A circle denotes the best-fit configuration related to Fit I. The resolution of the maps is 600×120 data points. Integrations are for $3 \cdot 10^4$ periods of the outer planet ($\sim 7 \cdot 10^4$) yr.

FIG. 3.— The solutions obtained with GAMP for the RV data from Vogt et al. (2005) for HD 128311. In the model, an inclined system and a 1:1 MMR is assumed. Orbital parameters are projected onto the planes of osculating elements. The smallest filled circles are for solutions with $(\chi^2_{\rm v})^{1/2}$ within the formal 3σ confidence interval of the best-fit (Table 1; $(\chi^2_{\rm v})^{1/2} < 1.9$ and the rms about 17 m/s). Bigger open circles are for $(\chi^2_{\rm v})^{1/2} < 1.825$ and $(\chi^2_{\rm v})^{1/2} < 1.81$ (2σ and 1σ confidence intervals, respectively). The largest circles are for the solutions with $(\chi^2_{\rm v})^{1/2} < 1.799$ marginally larger from $(\chi^2_{\rm v})^{1/2} = 1.797$ of the best-fit solution given in Table 1, Fit II. Compare the formal 3σ range for the solutions shown in the $(a_{\rm b}, a_{\rm c})$-plane with the width of the 1:1 MMR for the best-fit solution (Fig. 6, bottom row).

FIG. 4.— The synthetic RV curves for the best-fit solutions corresponding to the 2:1 and 1:1 MMRs in the HD 128311 planetary system (see also Table 1, Fits I and II). Thick line is for the 1:1 MMR and dashed line is for the 2:1 MMR. Both curves give an rms of $\simeq 15$ m/s. The error bars include the stellar jitter of 9 m/s.

FIG. 5.— The Lomb-Scargle periodogram for the best fit solutions found for the HD 128311 system (Fit I and II in Table 1). The thick line is for the synthetic RV corresponding to the 2:1 MMR. The thin line is for the RV curve of the 1:1 MMR solution. The dashed line is for the measurements.

FIG. 6.— The stability maps in the $(e_{\rm b}, e_{\rm c})$ (upper row, the resolution is 250×250 data points) and $(a_{\rm c}, e_{\rm c})$ plane (lower row, the resolution is 480×200 data points) for HD 128311 (Fit II). The left column is for the Spectral Number, $\log SN$. Colors used in the $\log SN$ map classify the orbits — black indicates quasi-periodic, regular configurations while yellow strongly chaotic systems. The maps marked with $\max e_{\rm c}$ and $\max\theta$ are respectively for the maximal eccentricity and the maximum of $\theta = \varpi_{\rm b} - \varpi_{\rm c}$ attained during the integration of the system. A circle marks the parameters of the best-fit solution. The integration was conducted for $\sim 6 \cdot 10^4$ orbital periods of the planets.

FIG. 7.— The stability maps in the $(e_{\rm b}, e_{\rm c})$-plane (the resolution is 250×250 data points) for the fit of the 1:1 MMR in the HD 128311 system having a slightly larger rms than the best-fit solution (Fit II in Table 1), $\simeq 15.7$ m/s and $(\chi^2_{\rm v})^{1/2} = 1.82$. The osculating elements at the date of the first observation are (m [m$_{\rm J}$], a [AU], e, i [deg], Ω [deg], ω [deg], M [deg]): (7.22, 1.730, 0.323, 43.52, 220.38, 80.18, 129.99) for the planet b and (2.83, 1.816, 0.582, 45.00, 0.00, 113.43, 312.87) for the planet c; $V_0 = -0.078$ m/s. The left column is for the spectral number, $\log SN$. Colors used in the $\log SN$ map classify the orbits — black indicates quasi-periodic, regular configurations while yellow strongly chaotic systems. The maps marked by $\max e_{\rm c}$ and $\max\theta$ are respectively for the maximal eccentricity of the outermost planet and the maximum of $\theta = \varpi_{\rm b} - \varpi_{\rm c}$ attained during the integration of the system. A circle marks the parameters of the best-fit solution. The integration was conducted for $\sim 6 \cdot 10^4$ orbital periods of the planets.

FIG. 8.— The stability maps in the $(e_{\rm b}, e_{\rm c})$ (upper row, the resolution is 250×250 data points) and $(a_{\rm c}, e_{\rm c})$ plane (lower row, the resolution is 400×200 data points) for HD 82943 (Fit IV, see Table 1). The left column is for the spectral number, $\log SN$. Colors used in the $\log SN$ map classify the orbits — black indicates quasi-periodic, regular configurations while yellow strongly chaotic systems. The maps marked by $\max e_{\rm c}$ and $\max\theta$ are respectively for the maximal eccentricity and the maximum of $\theta = \varpi_{\rm b} - \varpi_{\rm c}$ attained during the integration of the system. A circle marks the parameters of the best-fit solution corresponding to the 1:1 MMR in the HD 82943 system (Fit IV, Table 1). The integration was conducted for $\sim 6 \cdot 10^4$ orbital periods of the planets. The diamond at $(e_{\rm b} = 0.4, e_{\rm c} = 0.2)$ is for the initial condition in a discussion of the proper choice of the stability indicator in the GAMP-like code (see the Appendix).

FIG. 9.— The stability maps in the (e_c, ω_c)-plane of the HD 82943 system (the resolution is 240×240 data points) for the 2-planet edge-on best fit solutions related to the 2:1 MMR in the HD 82943 system. The top row is for the best stable Fit V (Table 2). The bottom row is for the alternative marginally worse solution with the following astrocentric elements $(m_p \sin i, a, e, \omega, M)$ at the epoch of the first observation: (1.781 m_J, 0.749 AU, 0.399, 118.273°, 0.000°) and (1.773 m_J, 1.194 AU, 0.012, 261.882°, 221.483°) for the inner and outer planet, respectively; an rms of this fit is ~ 8.1 m/s. The middle row is for 2-planet Keplerian Fit II of Lee et al. (2006). The left column is for the Spectral Number, $\log SN$. The colors used in the $\log SN$ map classify the orbits — black indicates quasi-periodic regular configurations while yellow strongly chaotic ones. The maps in the right column and marked with $\max e_c$ are for the maximal eccentricity of the outermost planet attained during the integration of the system. The circle marks the parameters of the best-fit solutions. The integrations were conducted for $\sim 4 \cdot 10^4$ orbital periods of the outermost planet.

FIG. 10.— The solutions obtained with GAMP for the RV data from Lee et al. (2006) for HD 82943. In the model, mutually inclined orbits and the presence of the 1:1 MMR is assumed. Orbital parameters are projected onto the planes of osculating elements. The smallest filled circles are for solutions with $(\chi^2_v)^{1/2}$ within the formal 3σ confidence interval of the best-fit (Fit VI in Table 2); $(\chi^2_v)^{1/2} < 1.55$ and the rms about 9 m/s. Bigger open circles are for $(\chi^2_v)^{1/2} < 1.46$ and $(\chi^2_v)^{1/2} < 1.45$ (2σ and 1σ confidence intervals, respectively). The largest circles are for the solutions with $(\chi^2_v)^{1/2} < 1.449$ marginally larger from $(\chi^2_v)^{1/2} = 1.447$ of the best-fit VI given in Table 2.

FIG. 11.— Evolution of MEGNO and orbital elements of the configuration described by Fit VI in Table 2. A perfect convergence of MEGNO over ~ 3 Myr indicates a rigorously stable solution. Subsequent panels are for the eccentricities, the critical argument of secular resonance θ and the relative inclination of orbits, i_{rel}.

FIG. 12.— The stability maps in the (e_b, e_c) (upper row, the resolution is 250×240 data points) and (a_c, e_c) plane (lower row, the resolution is 300×100 data points) for HD 82943 (Fit VI, see Table 2). The left column is for the spectral number, $\log SN$. Colors used in the $\log SN$ map classify the orbits — black indicates quasi-periodic, regular configurations while yellow strongly chaotic systems. The maps marked by $\max e_c$ and $\max \theta$ are respectively for the maximal eccentricity and the maximum of $\theta = \varpi_b - \varpi_c$ attained during the integration of the system. A circle marks the parameters of the best-fit solution corresponding to the 1:1 MMR in the HD 82943 system (Fit VI, Table 2). The integration was conducted for $\sim 3 \cdot 10^4$ orbital periods of the planets.

FIG. 13.— The Lomb-Scargle periodogram for the best fit solutions (Fit V and Fit VI, Table 2) found for the HD 82943 system. The thick line is for the synthetic RV corresponding to the 2:1 MMR. The thin line is for the RV curve of the 1:1 MMR solution. The dashed line is for the measurements from Lee et al. (2006).

FIG. 14.— The synthetic RV curves for the HD 82943 system. The top plot is for a stable (N-body) solution corresponding to a 2:1 MMR (Fit V). The middle plot is for the 1:1 MMR solution (Fit VI). The bottom plot is for stable Newtonian, 3-planet best fit solution (Fit VIII). The open circles are for the RV measurements from Lee et al. (2006). The error bars include stellar jitter of 4.2 m/s.

FIG. 15.— The stability maps in the (a_d, e_d)-plane of the HD 82943 system (the resolution is 300×120 data points) for the 3-planet Newtonian Fit VIII (Table 2). The left panel is for the Spectral Number, $\log SN$. Colors used in the $\log SN$ map classify the orbits — black indicates quasi-periodic regular configurations while yellow strongly chaotic ones. The right panel marked with $\max e_d$ is for the maximal eccentricity attained during the integration of the system. The circle marks the parameters of the best-fit solution (Fit VIII, Table 2). The integration was conducted for $\sim 6 \cdot 10^4$ orbital periods of the outermost planet.

FIG. 16.— Evolution of MEGNO and orbital elements of the 3-planet configuration described by Fit VIII in Table 2. A slow divergence of MEGNO after ~ 1 Myr indicates a marginally unstable solution. The evolution of the elements does not change over at least 250 Myr (not shown here). The subsequent panels are for the eccentricities, the critical angle of the 2:1 MMR and the semi-major axes.

FIG. 17.— The left column is for the evolution of MEGNO, $Y(t)$, and θ for the best-fit 1:1 MMR solution (Fit IV, Table 1) for HD 82943 . The right column is for the initial condition marked with a diamond in Fig. 8.

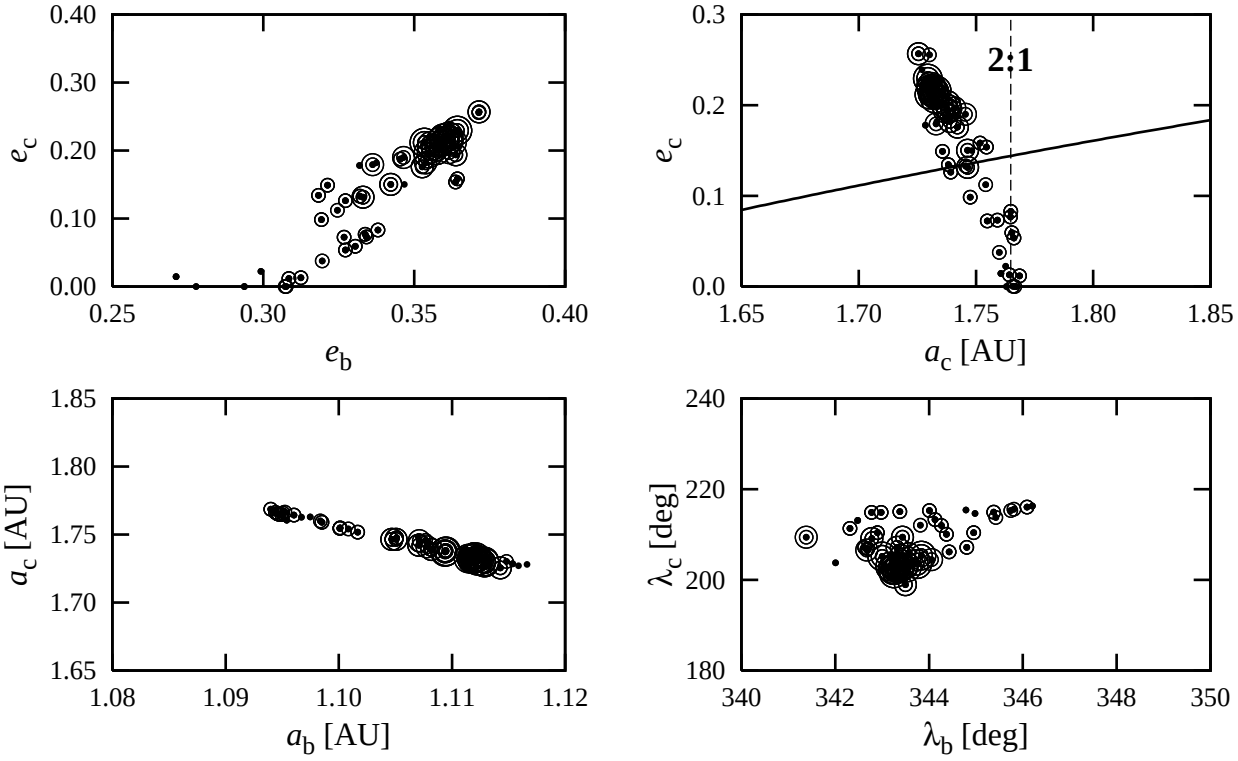
0.40
0.30
0.20
0.10
0.00
e_c
0.25
0.30
0.35
0.40
e_b
0.3
0.2
0.1
0.0
e_c
2:1
1.65
1.70
1.75
1.80
1.85
a_c [AU]
1.85
1.80
1.75
1.70
1.65
a_c [AU]
1.08
1.09
1.10
1.11
1.12
a_b [AU]
240
220
200
180
λ_c [deg]
340
342
344
346
348
350
λ_b [deg]

FIG. 1.—

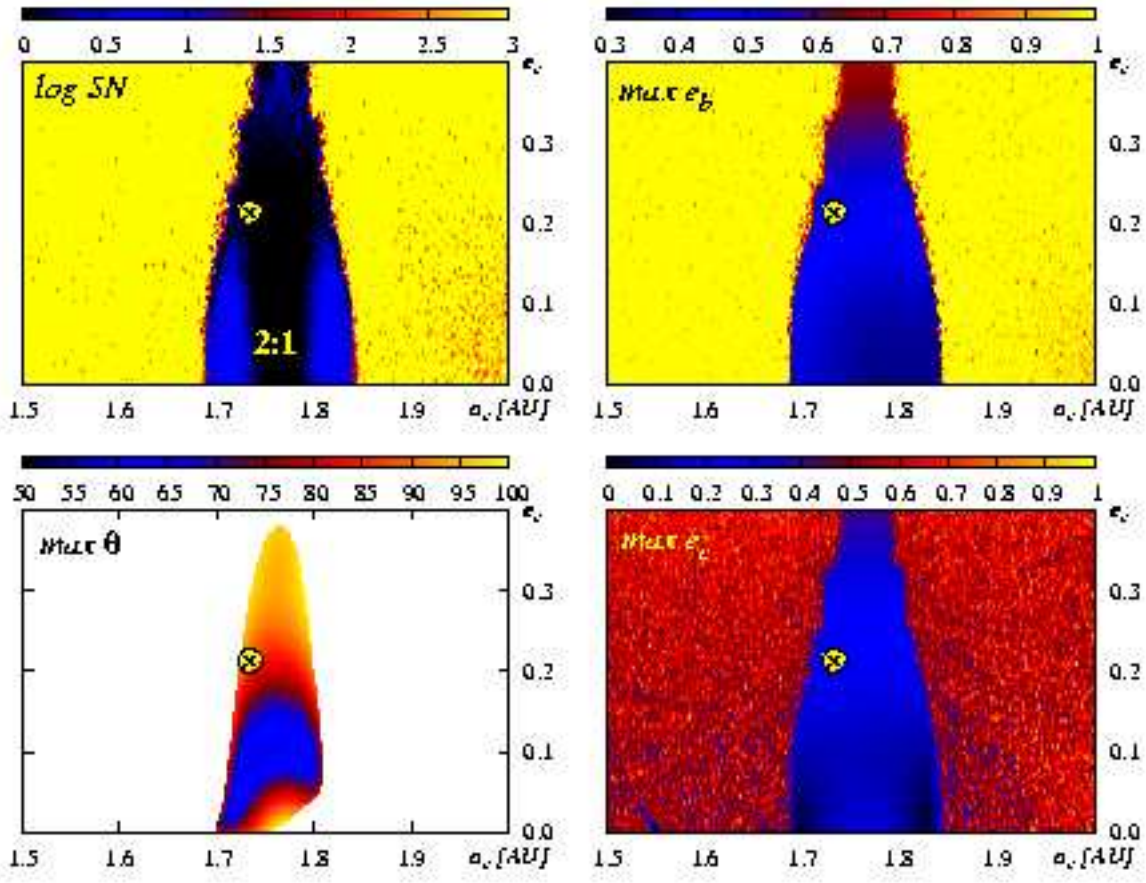
log SN
2:1
Max e_b
Max θ
Max e_c
a_c [AU]
e_c

FIG. 2.—

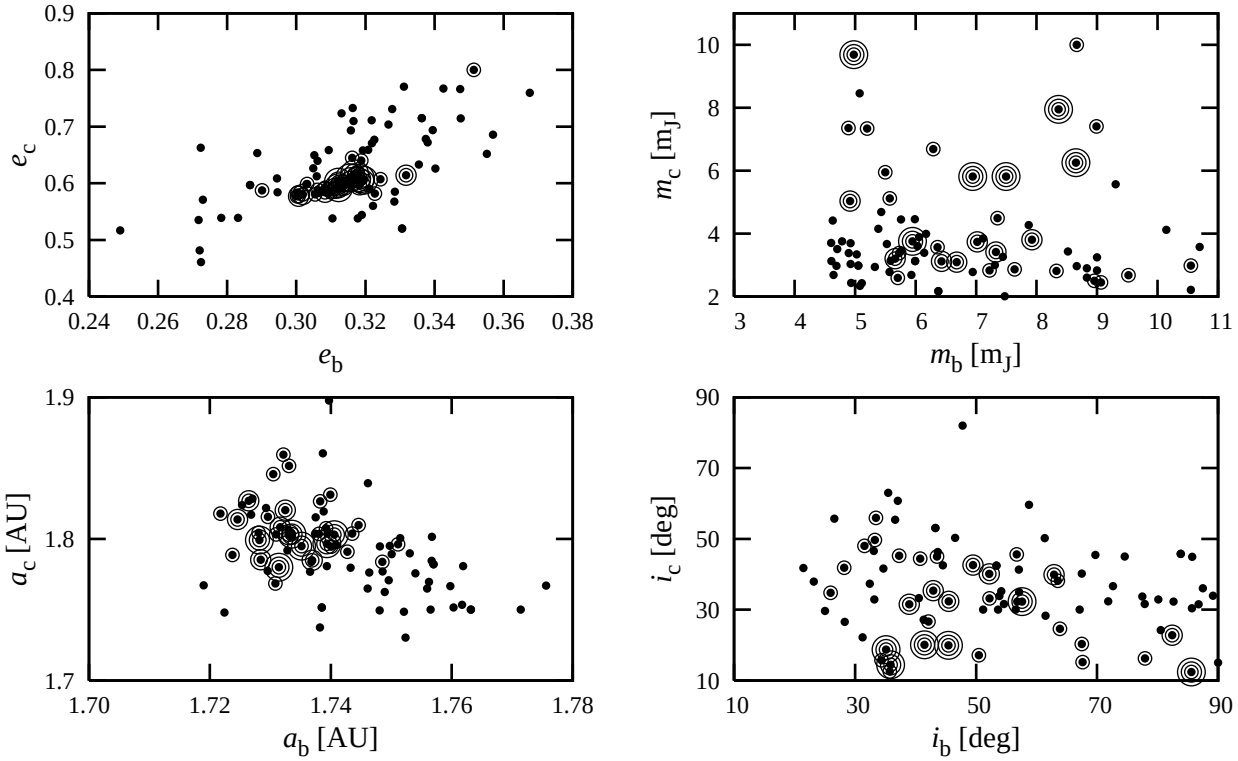
e_c
e_b
m_c [m_J]
m_b [m_J]
a_c [AU]
a_b [AU]
i_c [deg]
i_b [deg]

FIG. 3.—

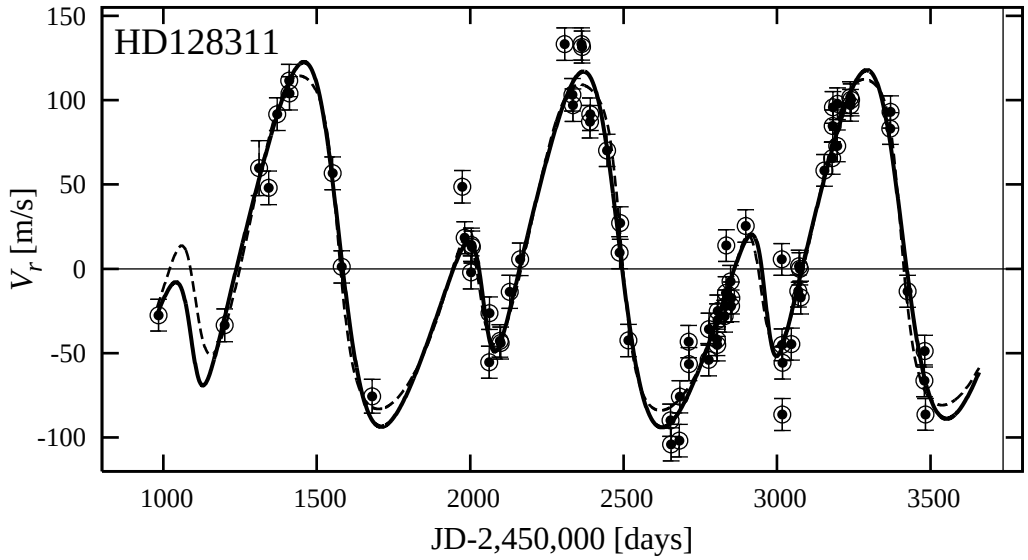
HD128311
V_r [m/s]
JD-2,450,000 [days]

FIG. 4.—

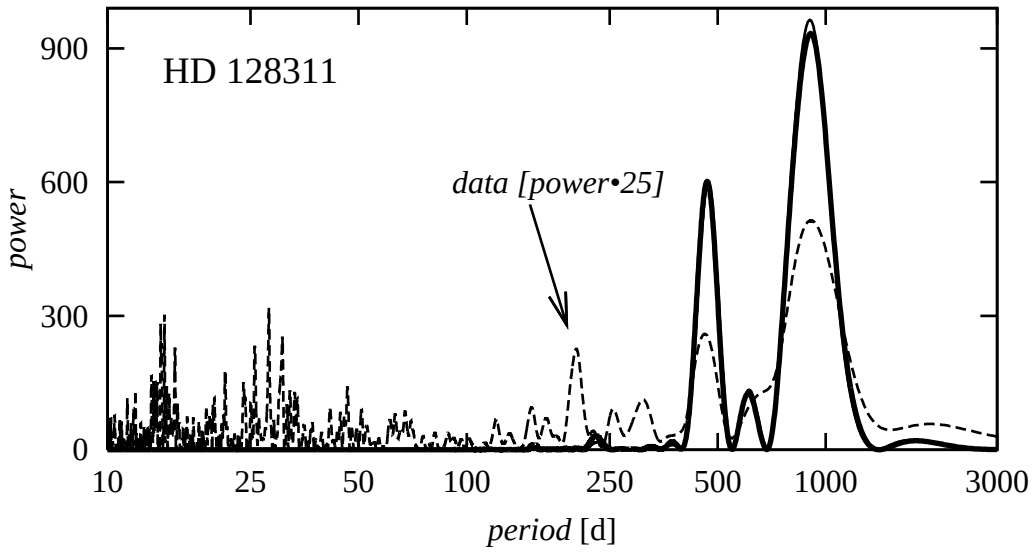
HD 128311
data [power•25]
power
period [d]
900
600
300
0
10
25
50
100
250
500
1000
3000

FIG. 5.—

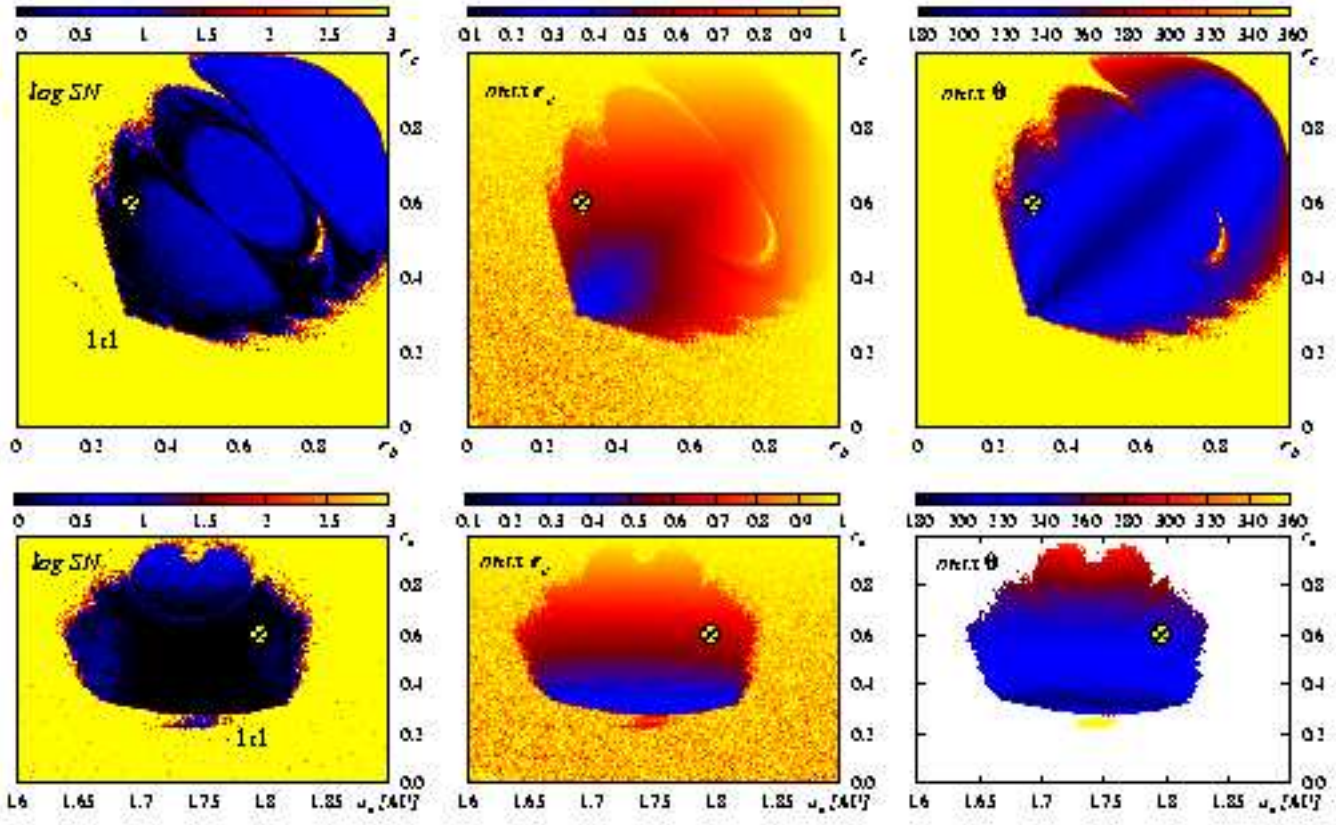
log SN
1:1
Figure 1:

FIG. 6.—

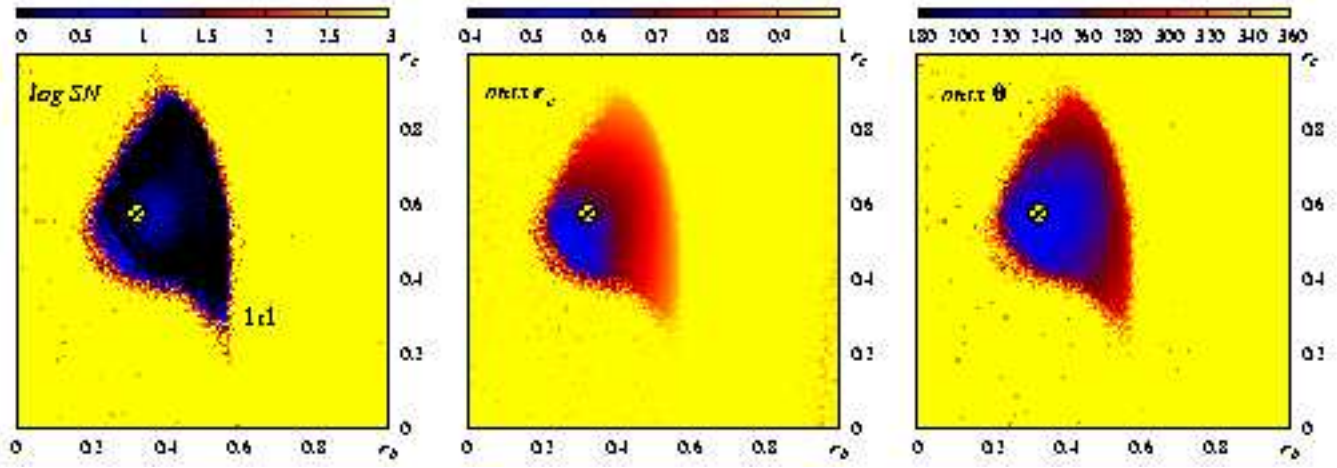

FIG. 7.—

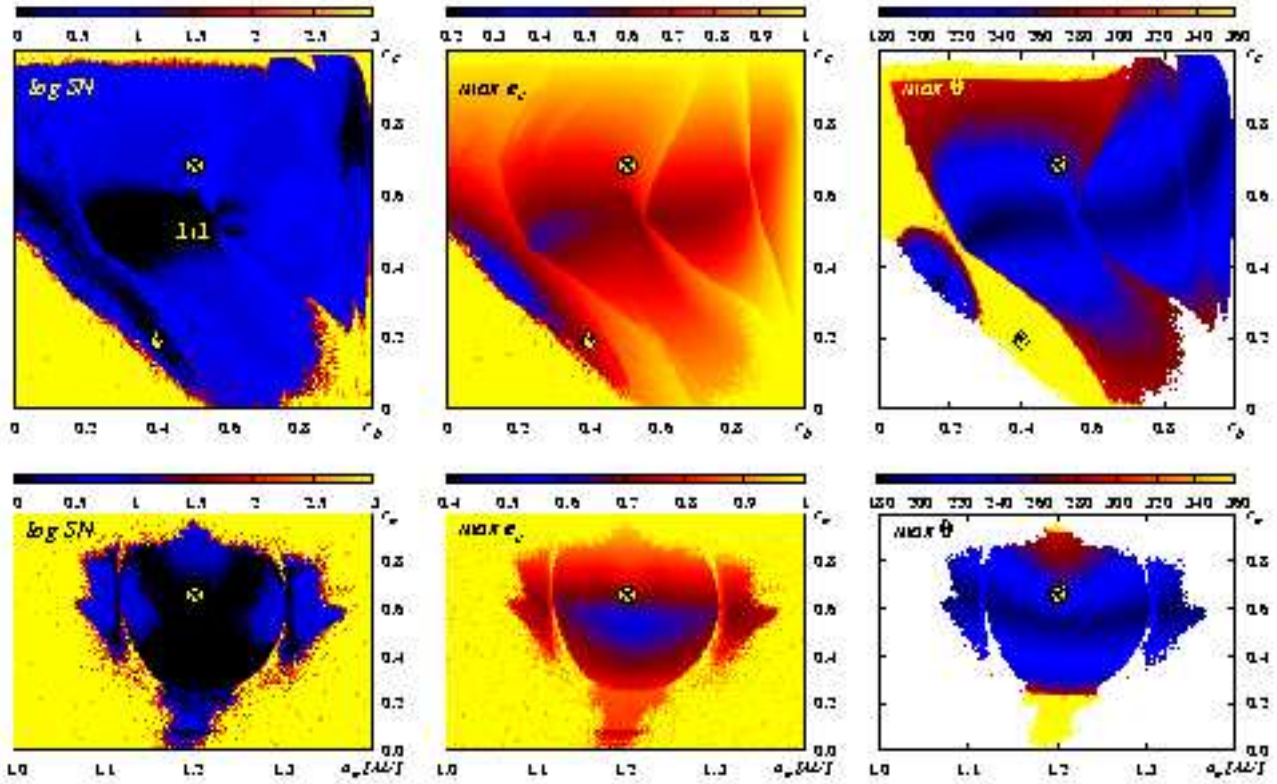

FIG. 8.—

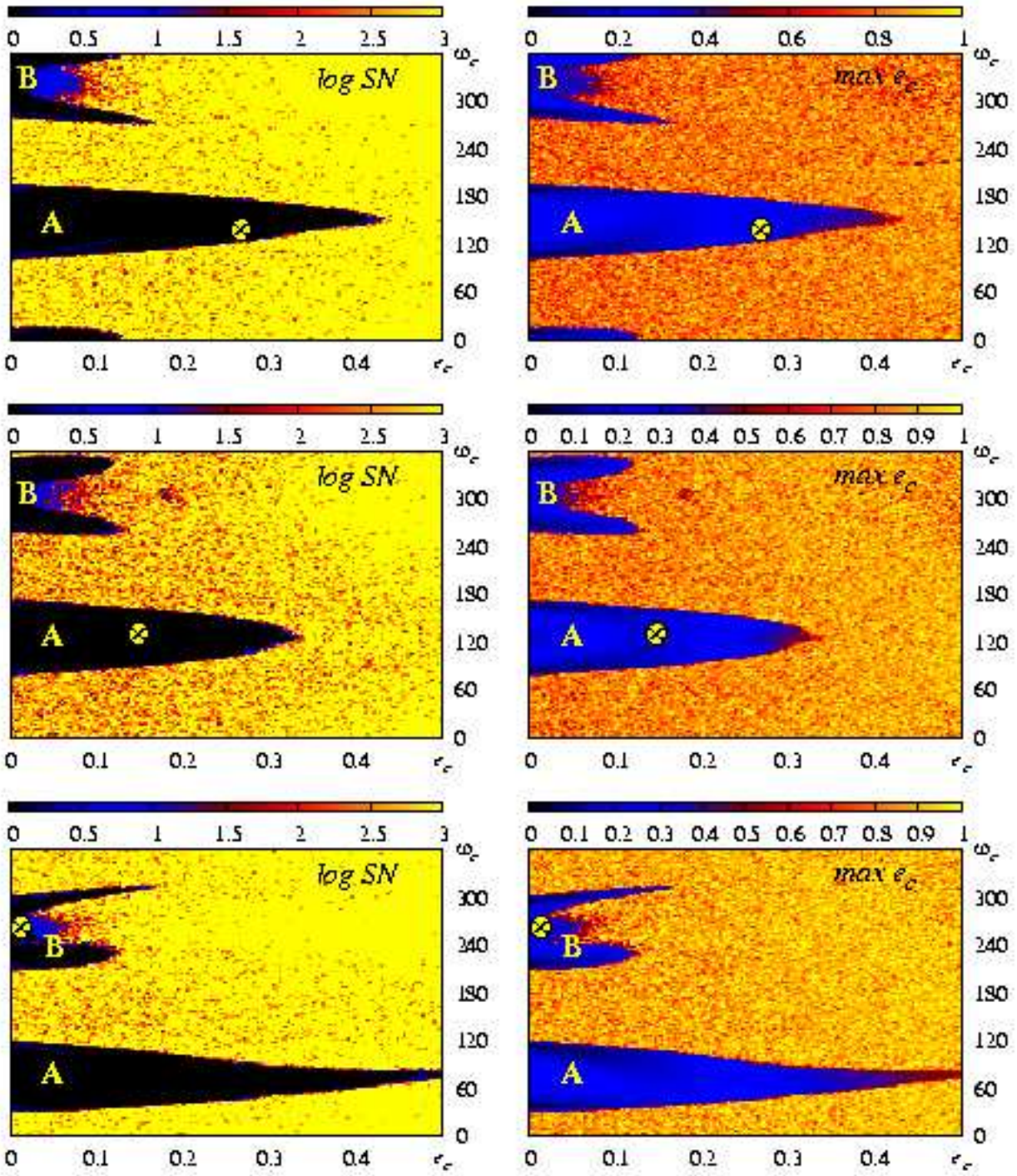
log SN
max ϵ_c
B
A
ω_c
ϵ_c
0 0.5 1 1.5 2 2.5 3
0 0.2 0.4 0.6 0.8 1
0 0.1 0.2 0.3 0.4 0.5 0.6 0.7 0.8 0.9 1
0 60 120 180 240 300
0 0.1 0.2 0.3 0.4

FIG. 9.—

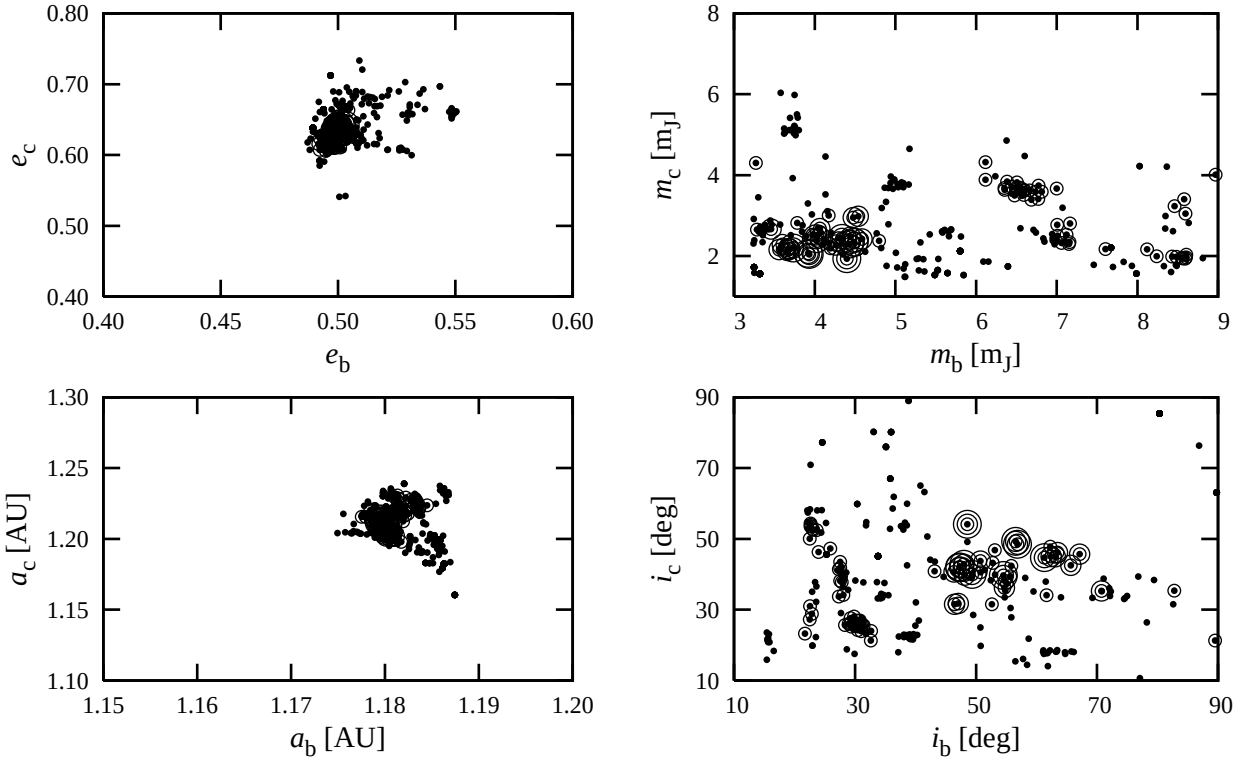
0.80
0.70
0.60
0.50
0.40
e_c
0.40
0.45
0.50
0.55
0.60
e_b
8
6
4
2
m_c [m_J]
3
4
5
6
7
8
9
m_b [m_J]
1.30
1.25
1.20
1.15
1.10
a_c [AU]
1.15
1.16
1.17
1.18
1.19
1.20
a_b [AU]
90
70
50
30
10
i_c [deg]
10
30
50
70
90
i_b [deg]

FIG. 10.—

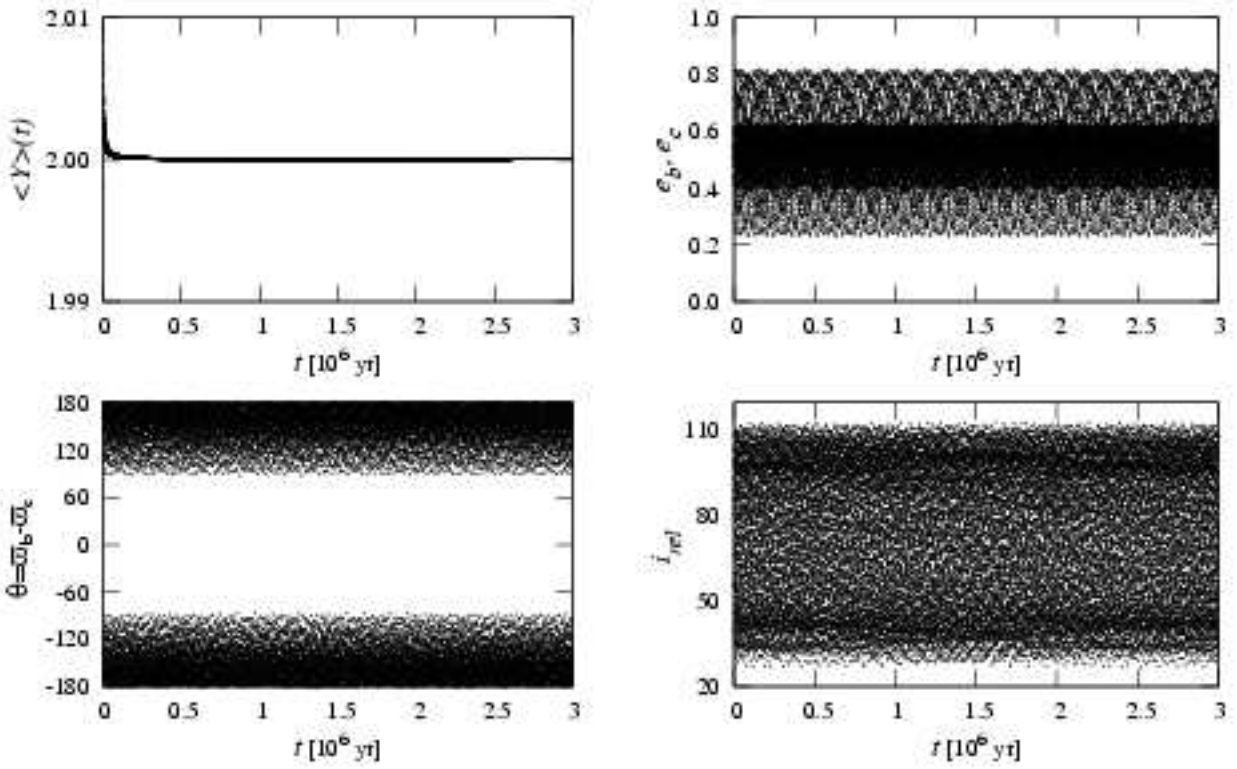
2.01
2.00
1.99
<γ>(t)
0
0.5
1
1.5
2
2.5
3
t [10^6 yr]
1.0
0.8
0.6
0.4
0.2
0.0
e_b, e_c
t [10^6 yr]
180
120
60
0
-60
-120
-180
θ=ϖ_b-ϖ_c
t [10^6 yr]
110
80
50
20
i_{rel}
t [10^6 yr]

FIG. 11.—

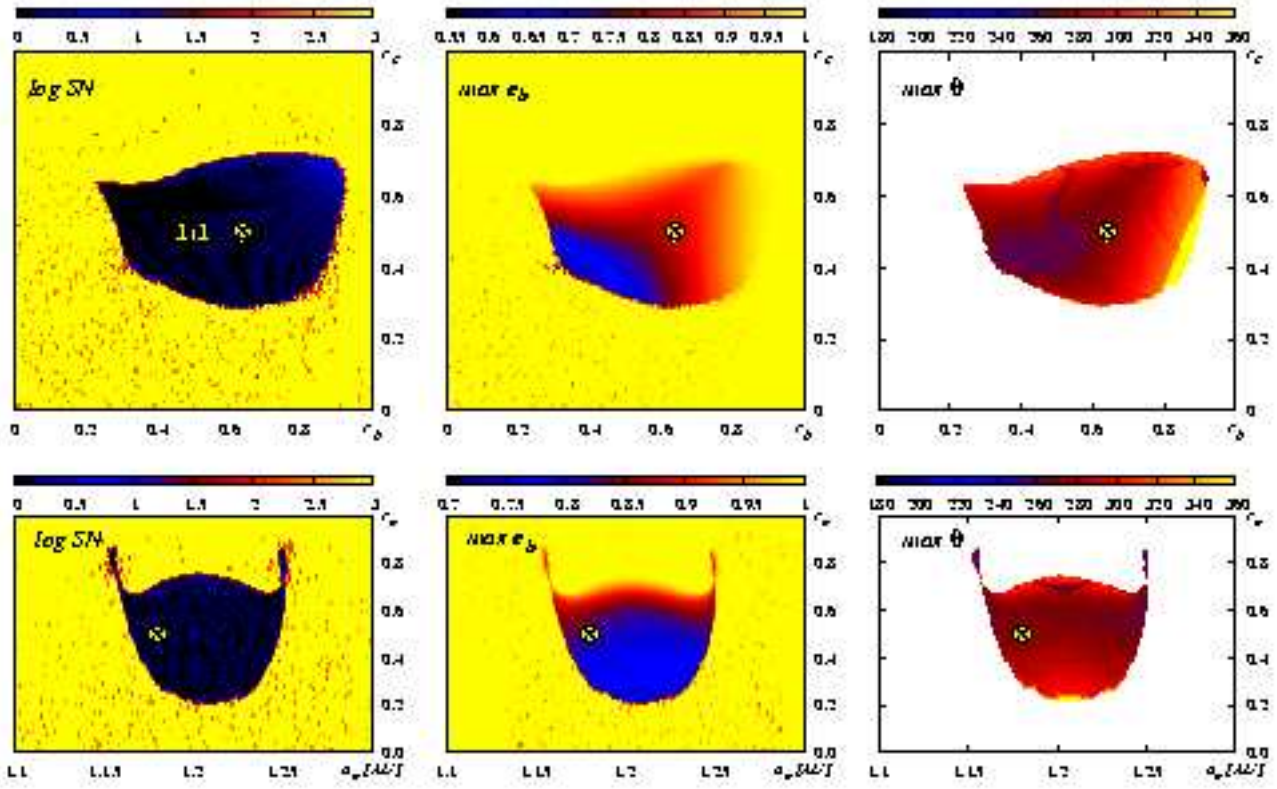
log SN
max e_b
max θ
1:1
log SN
max e_b
max θ

FIG. 12.—

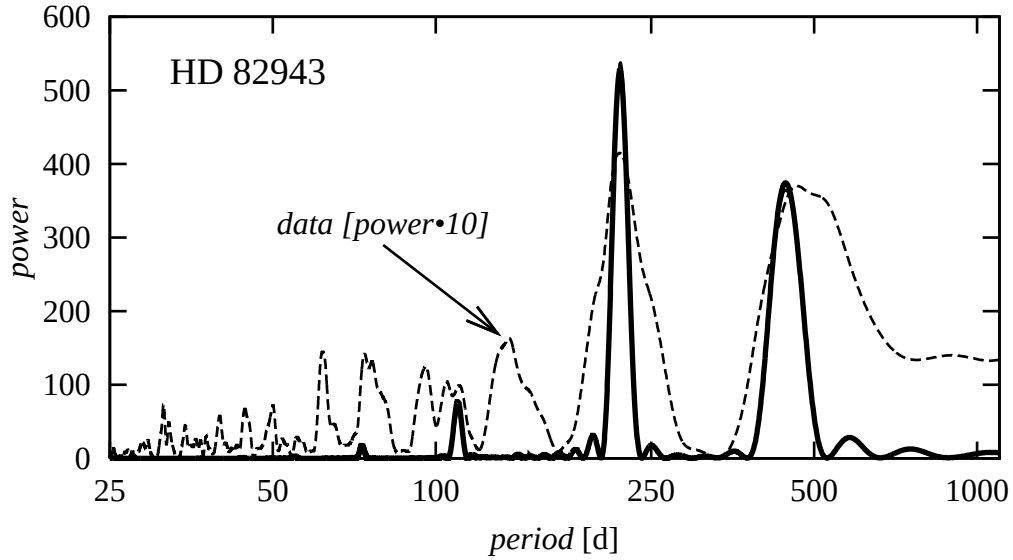
HD 82943
data [power•10]
power
period [d]
600
500
400
300
200
100
0
25
50
100
250
500
1000

FIG. 13.—

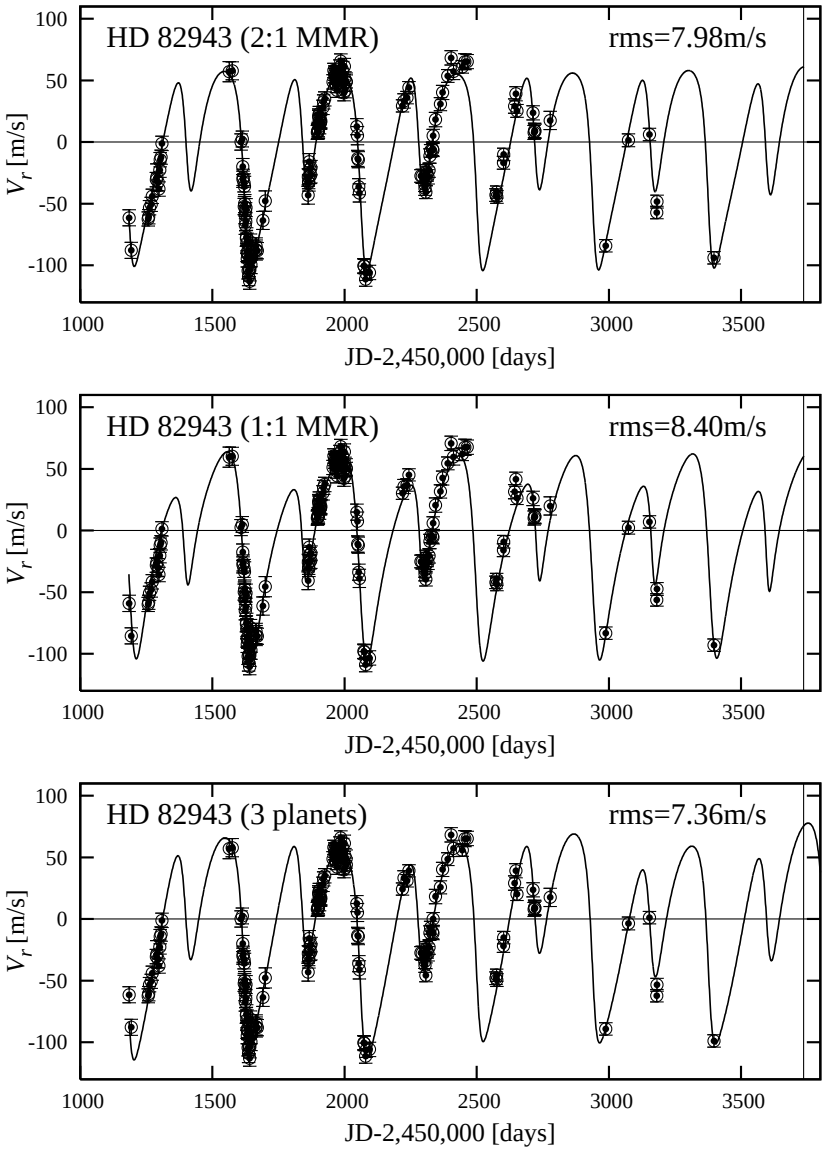
HD 82943 (2:1 MMR)
rms=7.98m/s
HD 82943 (1:1 MMR)
rms=8.40m/s
HD 82943 (3 planets)
rms=7.36m/s
V_r [m/s]
JD-2,450,000 [days]

FIG. 14.—

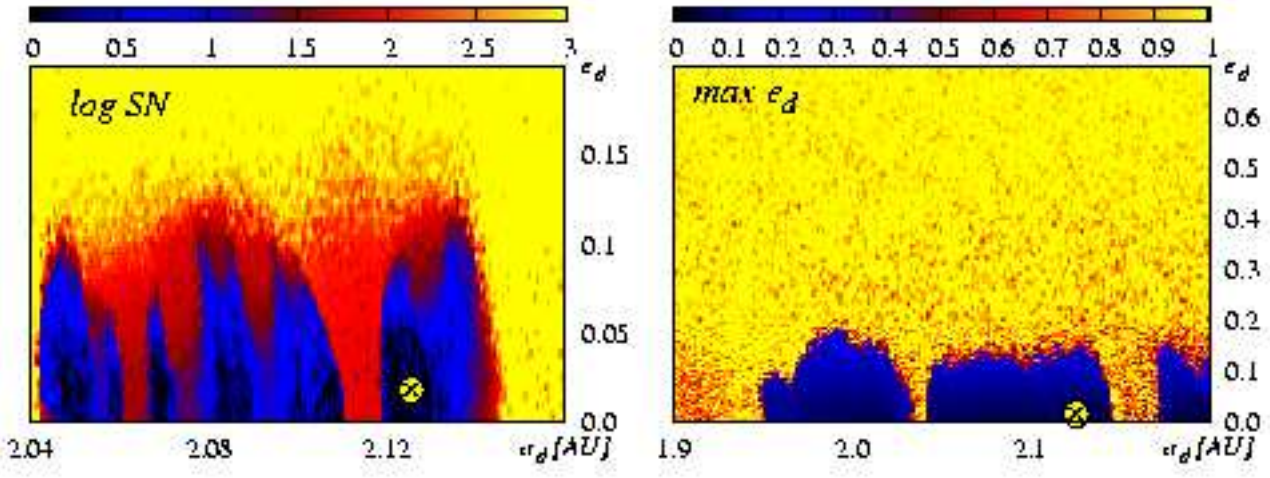
log SN
max e_d
e_d
a_d [AU]

FIG. 15.—

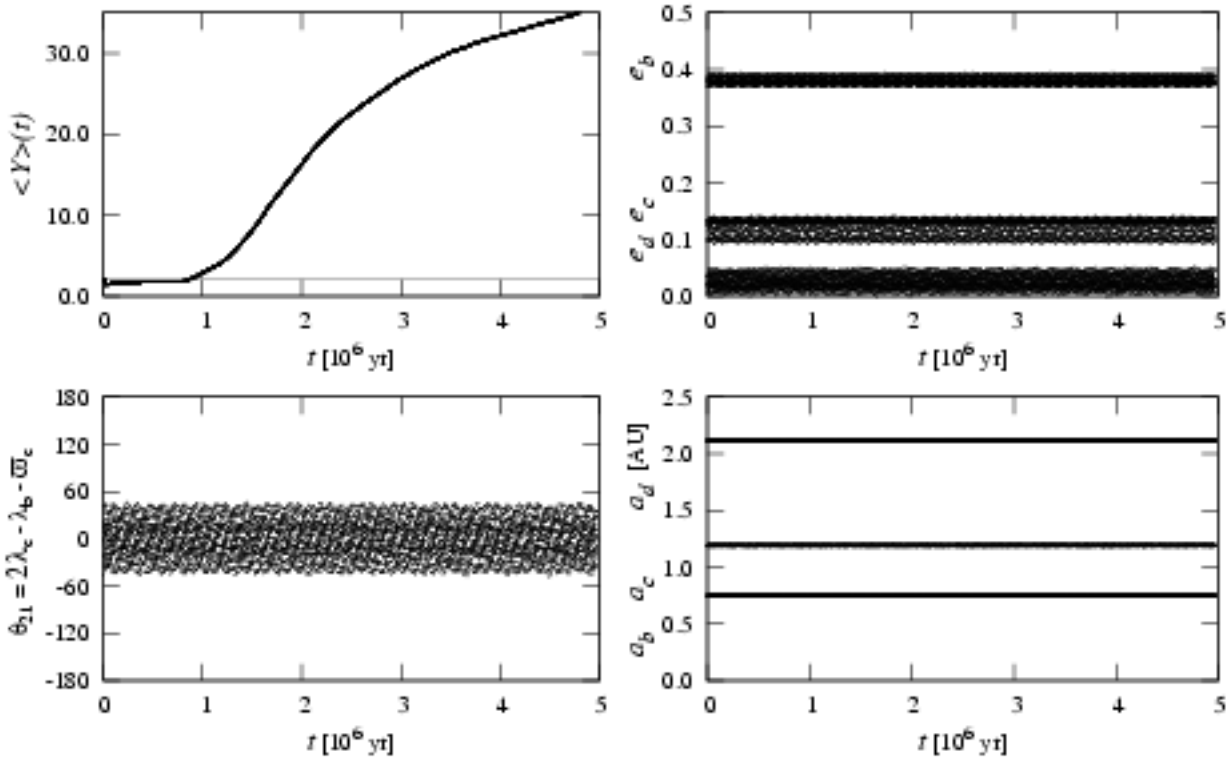

FIG. 16.—

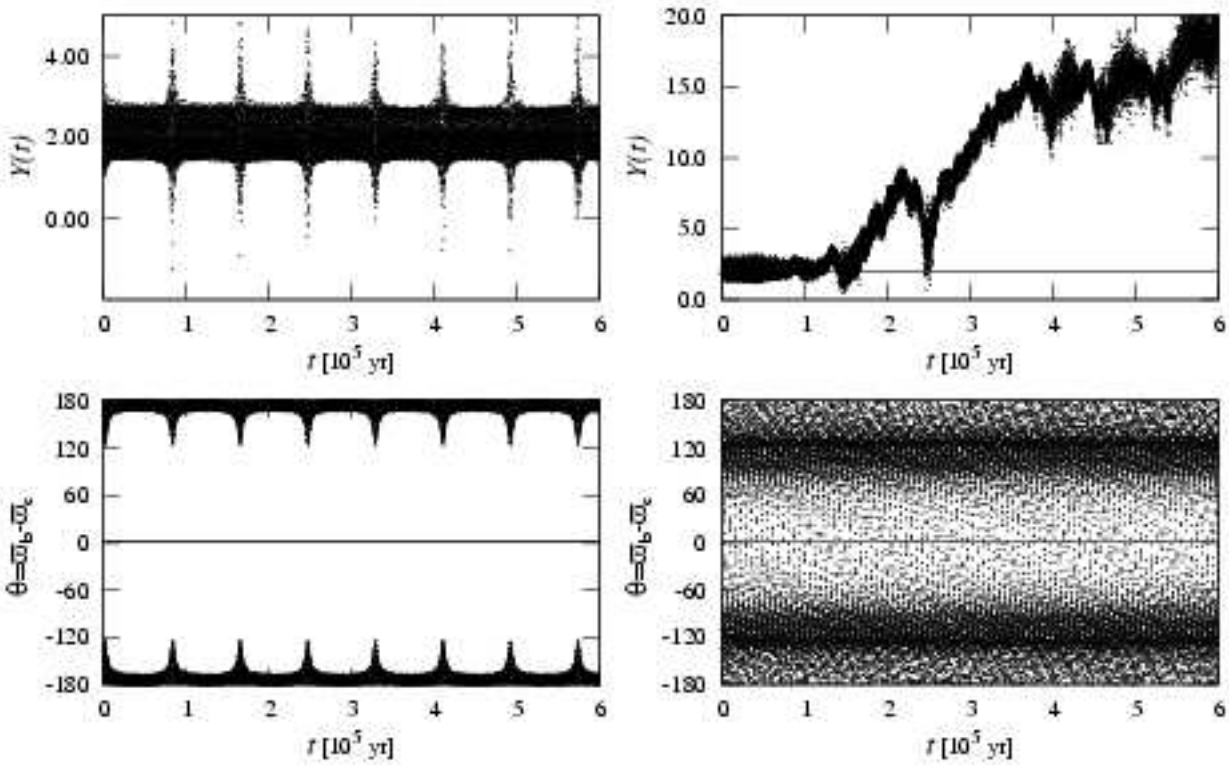

FIG. 17.—